

Title: A modified Jarvis-Stewart model for predicting stand-scale transpiration of an Australian native forest.

Number of Pages: 32

Number of Figures: 5

Number of Tables: 1

Corresponding Author: Rhys Whitley

Departments:

Institute for Water and Environmental Resource Management
Department of Environmental Sciences
Department of Physics and Advanced Materials

Address: University of Technology Sydney
P.O Box 123, Broadway
NSW, 2007
Australia

Phone No: (+61-2) 9514-2203

Fax No: (+61-2) 9514-2219

Email: Rhys.J.Whitley@student.uts.edu.au

A modified Jarvis-Stewart model for predicting stand-scale transpiration of an Australian native forest

Rhys Whitley^{1,2,†}, Melanie Zeppel¹, Nicholas Armstrong², Catriona Macinnis-Ng¹,
Isa Yunusa¹, Derek Eamus¹

¹*Institute for Water and Environmental Resource Management, University of Technology Sydney, Australia.*

²*Department of Physics and Advanced Materials, University of Technology Sydney, Australia.*

Abstract

Rates of water uptake by individual trees in a native Australian forest were measured on the Liverpool Plains, New South Wales, Australia, using sapflow sensors. These rates were up-scaled to stand transpiration rate (expressed per unit ground area) using sapwood area as the scalar, and these estimates were compared with modelled stand transpiration. A modified Jarvis-Stewart modelling approach (Jarvis 1976), previously used to calculate canopy conductance, was used to calculate stand transpiration rate. Three environmental variables, namely solar radiation, vapour pressure deficit and soil moisture content, plus leaf area index, were used to calculate stand transpiration, using measured rates of tree water use to parameterise the model. Functional forms for the model were derived by use of a weighted non-linear least squares fitting procedure. The model was able to give comparable estimates of stand transpiration to those derived from a second set of sapflow measurements. It is suggested that short-term, intensive field campaigns where sapflow, weather and soil water content variables are measured could be used to estimate annual patterns of stand transpiration using daily variation in these three environmental variables. Such a methodology will find application in the forestry, mining and water resource management industries where long-term intensive data sets are frequently unavailable.

Keywords: Jarvis model of transpiration; canopy conductance, woodland

[†] Corresponding author: Email address: rhys.j.whitley@uts.edu.au (R.J. Whitley)

29 **Introduction**

30

31 Measuring tree water use is an important step in determining the water balance of woody landscapes
32 (Komatsu et al. 2006a, Wullschleger et al. 2006, Rollenbeck et al. 2007, Simonin et al. 2007) and
33 determining landscape water balances is important to forestry and mining industries and to water
34 and landscape management agencies. Whilst estimating tree water use can be undertaken using
35 sapflow technologies (O'Grady et al. 1999, 2006), such measurements are made at the scale of
36 individual trees, usually over relatively short time frames (days and weeks) and typically only
37 during the growing season (Wullschleger et al. 1998, Lundblad and Lindroth 2002). However, to
38 obtain the required annual estimates of stand transpiration rate, up-scaling spatially and temporally
39 are required, even when there is continual monitoring of a few trees at a site. Whilst eddy covariance
40 measurements of stand water use give integrated measures of vegetation water use (Eamus et al.
41 2001, Ewers et al. 2007), these are expensive, technically challenging and require large, flat
42 homogenous landscapes. Key end-users of such annual estimates of vegetation water use, including
43 mine-site managers, catchment management authorities and water resource managers require a
44 methodology that is sufficiently robust to be useful, but not too resource (time, equipment, data)
45 intensive and one that is applicable to uneven terrain or small plots. An application of a simplified
46 model of vegetation water use, as applied to management of groundwater dependent ecosystems,
47 can be found in Howe et al. (2005).

48

49 Theoretically, in a well-coupled forest canopy, stand water use (E_c) can be calculated from canopy
50 conductance (G_c) and vapour pressure deficit (D) since $E_c = G_c D$ and $G_c = LAI G_s$ where LAI is
51 leaf area index and G_s is stomatal conductance (Whitehead 1998). G_s is a function of its driving
52 environmental variables and can be estimated using the non-linear, multiplicative, independent

53 functions originally described by Jarvis (1976) and subsequently widely applied (for example
54 Wright et al. (1995), Harris et al. (2004) and Komatsu et al. 2006a, b) and discussed by Whitehead
55 (1998). Thus, canopy water use can be calculated from:

56

$$57 \quad E_c = LAI G_s(R_s, D, \theta)D \quad (1)$$

58

59 for well coupled forests (Jarvis 1976, Whitehead 1998). This formulation is functionally equivalent
60 to the Penman-Monteith (PM) equation, yet is much simpler to fit, requires fewer measurements and
61 specifically avoids the circularity of inverting the PM equation to calculate G_c from E_c and then
62 using the PM again to estimate E_c from G_c , as has been applied in the past (Ewers and Oren 2000,
63 Lu et al. 2003, Pataki and Oren 2003). Furthermore, the PM is known to predict E_c poorly under soil
64 moisture limiting conditions (Zeppel 2006) and appears to correlate with observation best when E_c is
65 large (David et al. 1997, Rana et al. 2005).

66

67 The aim of the work contained herein is to describe a relatively simple model whereby scaled
68 estimates of stand water use can be made from measurements of a few environmental variables. Due
69 to its relative simplicity and practicality (Whitehead 1998, Wright et al. 1995, Harris et al. 2004), we
70 based our approach on the Jarvis-Stewart model (Stewart 1988) that requires only three parameters
71 and short-term measurements of sapflow. Jarvis-type models have been used extensively because of
72 their simplicity and they allow calculation of G_s as a function of meteorological variables and soil
73 moisture content (Jarvis 1976, Harris et al. 2004, Komatsu et al. 2006a,b, Ewers et al. 2007).
74 Stewart (1988) refined the Jarvis model to predict G_c which has since been applied to poplar trees
75 (Zhang 1997), maritime pine forest (Gash, 1989), oak forest (Ognick-Hendricks 1995), spruce and
76 pine forests (Lagergren and Lindroth 2002), an Amazonian pasture (Wright et al.1995) and

77 rainforest (Dolman et al. 1991, Sommer et al. 2002, Harris et al. 2004). The problem with the
78 application of J-S models to-date is that they require good estimates (high spatial and temporal
79 replication) of stomatal or canopy conductance and the subsequent use of the PM equation to
80 calculate transpiration rate.

81

82 We present the results from a field campaign that measured soil moisture content, net radiation, tree
83 water use, vapour pressure deficit and leaf area index, with the primary goal of scaling vegetation
84 water use without the need to measure either G_s or G_c and without, therefore, use of the PM
85 equation. We compare the model's output (E_C^{mod}) using our modified Jarvis-Stewart model (see
86 below), with the observed sapflow data (E_C^{obs}). Two modifications of the J-S model are described.
87 First, we model canopy water use directly without the intermediate calculation of G_c . Second, we
88 add leaf area index (LAI) to the model as LAI is an important determinant of water use and shows
89 seasonal and inter-annual variability (Eamus et al. 2006).

90

91 **Methods**

92 *Site description*

93

94 The study was conducted in remnant woodland within the Liverpool Plains, approximately 70 km
95 south of Tamworth, in north-western NSW (31.5 ° S, 150.7 ° E, elevation 390 m), as described by
96 Zeppel et al. (2004) and Zeppel and Eamus (2005). The open woodland has an average height of 15
97 m and is dominated by *Eucalyptus crebra* and *Callitris glaucophylla*. These two species contributed
98 approximately 75% of the tree basal area at the site. The total tree basal area at the site was $23.8 \pm$
99 $3.4 \text{ m}^2 \text{ ha}^{-1}$. The eucalypt population had a lower density than that of the *Callitris* (42 stems ha^{-1}

100 compared to 212 stem ha⁻¹) but contributed about 75 % of the basal area of the site because its
101 average diameter was much larger than that of the *Callitris*. Grasses including *Stipa* and *Aristida*
102 species dominated the understorey. Soils at the site were shallow (15 to 30 cm) with well-drained
103 acid lithic bleached earthy sands (Banks 1998) with occasional exposed sandstone.

104

105 The Liverpool Plains are characterised by summer dominant rainfall, as was evident during the
106 study period, when there were 19 rain events during January and late February. Maximum hourly
107 radiation reached 1342 W m⁻² in summer and vapour pressure deficit (VPD) averaged 1.4 kPa at
108 0900 h in February.

109

110 Radiation and temperature data were obtained from a weather station located in a cleared pasture (>
111 4 ha) approximately 100 m from the remnant woodland. Radiation, wet and dry bulb air
112 temperatures were recorded at hourly intervals. Wind speed was measured with a cup anemometer
113 located approximately 3 m above the canopy and soil moisture measured with Theta Probes
114 (Measurement Engineering Australia, Adelaide) at 10 cm, 40 cm and 50 cm depths at two locations,
115 and at 10 cm and 40 cm at one other location (8 Theta Probes in total). For the analyses presented
116 here, soil moisture measurements at 50 cm were used.

117

118 Leaf area index was measured at seven representative points in the woodland, as previously
119 described (Zeppel 2006) using a Li-Cor 200 Plant Canopy Analyser, on 10 occasions between
120 March 2003 and September 2004.

121

122 *Water use by individual trees*

123

124 The volume of water transpired by individual trees (Q ; $L d^{-1}$) was measured using commercial sap
125 flow sensors (model SF100, Greenspan Technology, Pty Ltd, Warwick, Australia) following the
126 procedures described previously (Zeppel et al. 2004). For each species 10-12 trees were chosen to
127 cover the range size distribution at the site and these were instrumented with 4 sensors per tree (2
128 probe sets per tree). The sensors were stratified with depth to account for previously measured
129 variation in sap flow across the radial profile of each tree (Medhurst et al. 2002; Zeppel et al. 2004)
130 and sensors were placed at 1/3 and 2/3 of the depth of the sapwood. Sapflows were corrected for the
131 effects of wound, radial variability in flow, sapwood area and volumetric fractions of water and
132 wood (Zeppel et al. 2004). Wound width was measured for both sensor sets in each of seven trees of
133 each species, as described by O'Grady et al. (1999), at the end of the sampling period. A wound
134 width of 2.5 mm for *C. glaucophylla* and 3.7 mm for *Eucalyptus crebra* was used to correct velocity
135 estimates. Basal area and diameter at breast height (DBH) of all trees were measured in 7 replicate
136 50 m x 50 m plots, as previously described (Zeppel et al. 2004).

137

138 *Scaling to stand transpiration*

139

140 Scaling from individual trees to stand transpiration required a number of steps. First, the relationship
141 between sapwood area and DBH was determined for each of the two species. Second, using the
142 *census* data of DBH for all trees within each of the 7 plots, the sapwood area of a hectare of the
143 stand was calculated by summing the sapwood area of the 2 species (ΣSA_{plot}). Third, an ANOVA
144 was conducted to determine whether there was a relationship between tree size (DBH) and sap
145 velocity. We found no relationship between tree size and sap velocity, as was observed in an
146 adjacent eucalypt plantation (Barton, pers. comm.). Consequently, the average hourly sap velocity

147 (SV_{plot}) for all trees measured with sap flow sensors was used to calculate total tree water use of the
148 plot, by multiplying total sapwood area of each plot by the average hourly sap velocity (Equation 2).
149 Each 24 hour period was summed to give the daily sap flux ($\text{cm}^3 \text{ day}^{-1} \text{ plot}^{-1}$).

150

$$151 \quad J_S = \sum (SA_{plot}) \times (SV_{plot}) \quad (2)$$

152

153 The water use ($\text{cm}^3 \text{ water d}^{-1} \text{ plot}^{-1}$) of each plot (with an area of 2500 m^2) was converted to stand
154 transpiration ($\text{mm}^3 \text{ of water d}^{-1} \text{ mm}^{-2} \text{ ground area}$).

155

156 The DBH of all trees in 7 replicate plots was measured and therefore there were 7 estimates of stand
157 water use ($\text{cm}^3 \text{ sap flux day}^{-1} \text{ cm}^{-2} \text{ ground area}$) for each day on which intensive field campaigns
158 was undertaken. The mean (and standard error) of all 7 plots, for each day, was then estimated, and
159 converted from $\text{cm}^3 \text{ water d}^{-1} \text{ cm}^{-2} \text{ ground area}$ to yield stand water use ($E_C, \text{mm d}^{-1}$).

160

161 *Modelling*

162

163 Stand water use ($E_C, \text{mm d}^{-1}$), was determined from functions of soil moisture content ($\theta, \%$), solar
164 radiation levels ($R_S, \text{W m}^{-2}$) and vapour pressure deficit (D, kPa). The functions (Fig. 2) were
165 modelled by their dependence between stand water use (estimated using Equation 1) and each of the
166 three driving environmental variables. Two modifications to the J-S model (Stewart 1998) have
167 been made in the present work. First, we model E_C directly (E_C^{mod}) rather than calculating G_c and
168 then using the PM equation to calculate E_c . Second, we include leaf area index in the model. Thus
169 E_C^{mod} can be expressed as a function of (R_S, D and θ).

170

171
$$E_C^{mod} = LAI E_{max} f_1(R_S) f_2(D) f_3(\theta) \quad (3)$$

172

173 E_{max} is defined as the observed maximum rate of stand transpiration for each driving variable and
174 LAI represents a site-specific leaf-area index term.

175

176 To determine the response functions for E_C in terms of its driving environmental variables, it is
177 assumed that the response of E_C to each variable is independent of the other variables when values
178 for the other variables are not limiting. This gives a set of functions expressing the separate
179 dependence of E_C on each of the driving variables. The functional forms of $f_1(R_S)$ and $f_3(\theta)$ for
180 this study were based on those of Stewart (1988), Wright et al. (1995) and Harris et al. (2004);
181 $f_2(D)$ is a new function based on measurements and observations made in a controlled environment
182 and tested in the field (Thomas and Eamus 1999, Eamus and Shanahan 2002, Zeppel 2006). The
183 functional forms for each of the independent variables are described below. The reader is referred to
184 San Jose et al. (1998), Magnani et al. (1998), Wullschleger et al. (2000) and Kosugi et al. 2007 for
185 examples of the application of these response functions.

186

187 The radiation response is described by Equation (4), and gives the form of an asymptotic increase
188 that plateaus at approximately 1000 W m^{-2} , with $k_1 (\text{W m}^{-2})$ describing the rate of change between E_c
189 and R_S .

190

191
$$f_1(R_S) = \left(\frac{R_S}{1000} \right) \left(\frac{1000 + k_1}{R_S + k_1} \right) \quad (4)$$

192

193 The functional form of $f_2(D)$ is:

194
195
196
197
198
199
200
201
202
203
204
205
206
207
208
209
210
211
212
213
214
215

$$f_2(D) = k_2 D^n \exp(-D/k_3), \quad n \in 1, 2, 3 \dots N \quad (5)$$

This vapour pressure deficit function (Equation 5), is a new term, modelled on the basis that the response observed shows a shape similar to that of the Boltzmann distribution. Most importantly this response function can replicate the three-phase response of transpiration plotted against stomatal conductance as D is increased from low to high values. Monteith (1995) has reviewed this topic and Eamus and Shanahan (2002) and Thomas and Eamus (1999) provide experimental and modelling verification. The parameter k_2 describes the rate of change at lower atmospheric demand up until a peak value, k_3 describes the rate of change at higher atmospheric demand and n is power term that may take on values 1, 2, 3... N and this can be restrained or free in the optimisation. For this study we have set $n=1$

The functional form of $f_3(\theta)$ is given by:

$$f_3(\theta) = \begin{cases} 0 & , \theta < \theta_w \\ \frac{\theta - \theta_w}{\theta_c - \theta_w} & , \theta_w < \theta < \theta_c \\ 1 & , \theta > \theta_c \end{cases} \quad (6)$$

Equation (6) shows the soil moisture response to be a three-phase relationship, where θ_w and θ_c denote the wilting point and critical points respectively, of the relationship between water use and soil moisture content.

Maximum likelihood estimation

216

217 A full multivariate optimisation was applied to the experimental (measured) data using ordinary
218 least squares (OLS). For an OLS regime to be valid, the variance must be homoscedastic (constant
219 variance with increasing measurement). In cases where the data is seen to be heteroscedastic
220 (increasing variance with increasing measurement) weighted least squares must be used in order to
221 account for the increasing uncertainty in the measurement. A weighted least squares criterion uses a
222 weighting term in the fitting regime in order to account for the heteroscedasticity of the data. By
223 including a weighting term, the changing uncertainty in the measurements can be accounted for and
224 the optimised free parameters will be maximum likelihood.

225

226 The parameters k_1 , k_2 , k_3 , θ_W and θ_C are the optimised free parameters that represent response
227 constants in the Jarvis-Stewart model. These response functions give values between 0 and 1, and
228 hence the product of these functions act as scaling terms, which are used to reduce a maximum
229 transpiration term (E_{max}) to an ‘actualised’ value E_C^{mod} (mm d^{-1}). Optimisation of Equations 4 - 6
230 was done by taking the weighted sum of the square of residuals ($WSSR$), given k_1 , k_2 , k_3 , θ_W and θ_C
231 set at starting values based on visual observations of the relationships and field measurements.

232 Where we express the $WSSR$ as:

233

$$234 \quad WSSR = \sum \left(\frac{y_i - \hat{y}_i}{\sigma_i} \right)^2 \quad (9)$$

235 where

$$236 \quad \sigma_i = \beta y_i \quad (10)$$

237

238 where y_i is the i th experimental value E_C^{obs} \hat{y}_i is the i th predicted value based on the equation fitted
239 to the data and σ_i where ‘ i ’ is the i th standard deviation.

240
241 We presuppose the heteroscedasticity to be explained by Equation (10), expressing the standard
242 deviation to be proportional to the experimental data y_i , multiplied by some constant of
243 proportionality β . In order to specify whether σ_i is normally distributed, we have assumed that the
244 residuals to be some surrogate for σ_i such that $(y_i - \hat{y}_i) \equiv \sigma_i$. For this study we assume random
245 measurement error (σ_i) to be normally distributed and heteroscedastic based on observations of the
246 weighted residuals (Fig. 3).

247

248 *Filtering the Data Set*

249

250 Daily measurements of sapflow were filtered to exclude hours when solar radiation was zero (night).
251 Days with rainfall events were also excluded to avoid wet-canopy conditions. This filtered data-set
252 were used to define the boundary conditions for equations (4), (5) and (6).

253

254 To avoid circularity (using the same data to both parameterise the model and to compare with model
255 outputs), the 59 day period of measurements during Jan-Feb were partitioned into two separate data
256 sets of alternate days. The first data set (days 1, 3, 5) was used to optimise the seasonal response
257 parameters, and the second data set (days 2, 4, 6) was used to validate the model. It was found
258 that no systematic patterns with a day variation were evident in the data and there was no change in
259 model outputs when allocation of each half of the data set to either optimisation or validation was
260 reversed.

261

262 **Results**

263 *Weather variables, soil moisture content, LAI and scaled rates of stand water use*

264

265 Mean daily values for R_S , D , θ and E_C show daily fluctuation over the 59 day period (Fig. 1a-c).

266 Variation in daily mean stand transpiration varied up to 8 fold between consecutive days. Mean

267 daily scaled stand transpiration (scaled by sapwood area) varied between 0.1 mm d^{-1} during a rainy

268 day (24th Feb) and approximately 2.8 mm d^{-1} (Feb 28th) on a rain free day. Declining stand water use

269 between the 4th Feb and 22nd Feb was associated with declining soil moisture content, whilst large

270 increases in stand water use occurred after the 13th Jan and after 24th Feb following rain events and

271 soil moisture increased.

272

273 The three largest rainfall events increased soil moisture at 50 cm depth (Fig. 1c) but smaller rain

274 events did not influence soil moisture at this depth. Daily mean vapour pressure deficit ranged from

275 about 0.1 kPa on a rainy day to almost 6 kPa (20th Feb) after a period (17 days) with very little (< 6

276 mm) rain in summer (Fig. 1a). Leaf area index varied between 0.9 in March 2004 and 1.5 in March

277 2003 but was typically in the range 0.8 to 1.2 (data not shown).

278

279 Figure 2 shows the functional forms of the curves described by equations 3 - 5 respectively, fitted to

280 the experimental data. Note that the independent variable is a scaled stand water use, with a range

281 from zero to one. Similar forms to these responses can be observed in Kelliher et al. (1993) and

282 Komatsu et al. (2006b). These boundary curves show that as solar radiation increased, stand water

283 use increased from zero to a maximum, asymptotically, whilst increasing vapour pressure deficit (D)

284 caused stand water use to increase for low values of D as evaporative demand increases, shows
285 minimal change in water use for a narrow intermediate range of D and then declines with increasing
286 D beyond this narrow range ($D > 3$ kPa). Stand water use showed a three phase response to soil
287 moisture content. At high values of soil moisture (above the field capacity), stand water use was
288 independent of soil moisture content. As soil moisture content declined below field capacity, stand
289 water use declined linearly, as has been described previously (Harris et al. 2004). At very low soil
290 water content, stand water use was zero.

291

292 *Modelled stand water use*

293

294 A total of six free parameters were estimated using a multivariate weighted least squares regime.
295 Minimisation of the $WSSR$ was done using *Mathematica*®, producing a set of optimised parameter
296 values best describing the seasonal responses. The optimised parameters, as well as their standard
297 errors are shown in Table 1. The residuals between E_C^{obs} and E_C^{mod} (Fig. 3) revealed a minor
298 heteroscedasticity of the data, as is made evident by the slight pattern of the residuals. In order to
299 properly account for this, we used a weighted least squares approach and Equation 9 was thus
300 optimised. A weighted least squares approach was considered to be viable as the random errors in
301 the measurements were seen to be normally distributed assuming a Gaussian distribution. Thus the
302 six free parameters were considered to be maximum likelihood. The seasonal response parameters
303 were used in the full form of Equation (3) to give E_C^{mod} ; a set of predicted stand transpiration values.

304

305 The estimated maximal value for E_{max} of 0.260 mm hr^{-1} is very close to, yet under the observed
306 maximal value of 0.280 mm hr^{-1} . This suggests that the model may slightly under-predict stand
307 transpiration (Fig. 4) over the January-February period. This can be considered acceptable, as the

308 model does not predict night-time transpiration due to the radiation component of the model. There
309 are also two short periods where the model has failed; these are 15th-16th Jan and 25th-29th Feb where
310 large rainfall events occurred. The weighted sum of modelled stand water use for the split 59-day
311 period was 40.13 mm whilst the measured water use was 42.0 mm (data not shown). As only half
312 the days were parameterised, these total values can be assumed to be 50% of the January-February
313 total stand water use. The weighted mean for modelled stand water use was 1.38 mm d⁻¹ and for
314 measured stand water use it was 1.62 mm d⁻¹. Fig. 4 shows the outputs of our modified Jarvis-
315 Stewart model. The regression of the observed and modelled rates of stand water use has a slope of
316 0.96 and an R² of 0.9 (Fig. 5). Values for $\theta_w = 6.72\%$ and $\theta_c = 11.79\%$ are also close to the
317 graphically observable points shown by the scattering plot in Fig. 2c. This indicates further that the
318 modelling is producing a reasonable description of the observed data (Table 1).

319

320 **Discussion**

321

322 As solar radiation increases, stand water use increased from zero to a maximum, asymptotically.
323 Hyperbolic saturating functions to canopy conductance or water use have been applied extensively
324 at leaf, tree and canopy-scales (Kelliher et al. 1993, Granier et al. 2000). At low levels of incident
325 radiation, energy supply limits evaporation, but at high levels of radiation, other factors (especially
326 soil moisture content and hydraulic conductance of soil and plant), limit evaporation (Williams et al.
327 1998). In agreement with Sommer et al. (2002) and Harris et al. (2004) we found that incorporating
328 the soil moisture response function was critical to the ability of the model to satisfactorily fit the
329 observed data.

330

331 The response of stand water use to increasing vapour pressure deficit (D) was more complex than
332 that observed for radiation. For low values of D , increasing D resulted in stand water use increasing
333 as evaporative demand increased. For a narrow range of D ($3 \text{ kPa} > D > 2 \text{ kPa}$), a minimal change
334 in stand water use occurred as D increased. For large values of D ($D > 3 \text{ kPa}$) stand water use
335 declined with increasing D . This three-phase behaviour of stand water use is comparable to that of
336 stomatal behaviour observed at the leaf-scale (Monteith 1995, Thomas and Eamus 1999, Eamus and
337 Shanahan 2002) and of canopy conductance (Pataki et al. 2000, Komatsu et al. 2006b, Zeppel 2006).
338 The initial response of E_C to increasing D for low values of D is unlikely to be a response to the
339 covariance of R_s in the morning because even under a constant, saturating level of light, the same
340 three-phase behaviour was observed (Thomas and Eamus 1999). The threshold of 2 – 3 kPa
341 observed in the present study is larger than that observed in Pataki and Oren (2003) and Komatsu et
342 al. (2006b) and the decline in water use was more severe than the decline in G_C they observed. This
343 is probably because the site used in the present study is much drier, experiences a much larger range
344 of D and was recovering from a long period of drought, compared to those used by Pataki and Oren
345 (2003) or Komatsu et al. (2006b). The response of stomata (and hence water use) to D is strongly
346 influenced by soil moisture content and drought (Thomas et al. 1999, 2000).

347

348 With some exceptions, the response of stand water use to increasing D did not fully describe the
349 relationship shown in Figure 2 b) in terms of its boundaries. Whereas Equations (3) and (5) describe
350 a normalised function of values between 0 and 1, Equation (4) does not due to the model being
351 based on a distribution function, i.e. values are not restricted to boundary conditions $0 < f_2(D) < 1$,
352 and may fall outside this region depending on the choice of starting values and the optimisation
353 itself. This undoubtedly causes problems in the optimisation with the free parameters k_2 and k_3 ,
354 perhaps not accurately describing the relationship between E_C and D . However the function does

355 appear to describe the observed data with reasonable precision and has practical applications in the
356 full model. Future work is required to develop a clear functional form of the response of water use to
357 D .

358

359 The pattern of variation in measured hourly stand water use (Fig. 4) reflected changes in solar
360 radiation and D and the model was able to capture this variation even at hourly time-scales. For
361 example, the interval 9th – 18th Jan encompassed a period where observed hourly stand water use
362 varied 12 fold because of the rainfall that occurred during this period. The model was able to
363 replicate this range and the time course of the response of stand water use to fluctuations in solar
364 radiation, D and soil moisture content that occurred before, during and after the rainfall. Similarly,
365 more gradual declines in the maximum rate of stand water use that were observed during drying
366 periods (late Jan to late Feb) were captured in the model. The ability of the model to capture this
367 variability is further supported by the regression of E_C^{obs} and E_C^{mod} which produced a slope of 0.96
368 (Fig. 3), whilst the optimised observed daily maximum E_C^{obs} (0.280 mm h⁻¹) and modelled E_C^{mod}
369 (0.260 mm h⁻¹) were very close. Unlike the use of the PM equation, this model appeared to be
370 equally applicable to conditions of low and high E_c , and at hourly or daily time-steps, making it
371 generally more applicable than the PM equation, which appears to be less successful under
372 conditions of low E_c or hourly time-steps (David et al. 1997, Rana et al. 2005, Whitehead 1998).

373

374 Optimisation problems have been noted in using an OLS criterion, with the obvious problem of a
375 large 6-dimensional parameter space. By increasing the number of functions and hence the number
376 of free parameters, the complexity of the problem increases. As a consequence, the optimisation
377 must cover a large, complex parameter space in order to find the global minimum that equates to the
378 maximum likelihood for all free parameters. Problems of local minima hamper the search by

379 causing early convergences over the large parameter space. This is a hindrance in determining
380 values for the free parameters best describing the seasonal response, and will overall have an effect
381 on the outcome of the model. Due to the sensitivity of the optimisation, there are also problems in
382 choosing starting values for the free parameters. In order for the optimisation to converge close to
383 the perceived global minimum, the starting values must be close to an observable value. A possible
384 solution to these problems is by using heuristic search algorithms such as simulated annealing or
385 genetic algorithms, which cover the entire parameter space with all possible solutions. These
386 solutions evolve and undergo a simulated process of natural selection until the best solution is
387 found. Although heuristic search algorithms can be applied to these high dimensionality problems,
388 they are only acquiring part of an underlying distribution that describes these seasonal response
389 parameters. A more desirable method of parameterising this model would be the application of
390 Monte Carlo Markov Chain (MCMC) techniques such as those used by Richardson and Hollinger
391 (2005). By acquiring a distribution for each parameter and hence a mean and standard deviation, a
392 better understanding of the seasonal responses can be obtained. This is seen as the next step in this
393 analysis.

394

395 This model has been applied to a single season (summer) at a single site. In the future we will
396 compare summer and winter data at this site to determine the extent to which parameter values vary
397 between seasons and investigate the requirement for a temperature response function in this model.
398 Komatsu et al. (2006b) demonstrate the need for a temperature response function to extend the
399 models to annual time-frames. Clearly, within the single summer season used in this paper, the
400 temperature response function was not required because of the relatively narrow range of
401 temperatures experienced during the day.

402

403 **Conclusions**

404

405 For this study a Jarvis-Stewart model has been modified to investigate whether stand-scale water use
406 can be estimated from incident solar radiation, vapour pressure deficit and soil moisture content in
407 conjunction with a limited number of sapflow measurements (30 days) made over a 2 month period.
408 Functional forms of the Jarvis-Stewart functions were found to adequately describe the response of
409 stand water use to variation in solar radiation, vapour pressure deficit and soil moisture content.
410 Despite having only 30 days of sapflow data (half of the 59 day study period) with which to
411 parameterise the model, the regression of modelled *versus* observed stand water use had a slope of
412 0.96 and an R^2 of 0.90. Thus the model has been shown to work well, with an acceptable level of
413 error between experimental and modelled measurements. Some of the uncertainty present in the
414 measurements has been accounted for by considering a weighting term in the optimisation of the
415 model and gave a slight improvement over an unweighted optimisation.

416

417 In the case of the D relationship a new functional form was developed to incorporate the three-phase
418 response of stomatal or canopy conductance to changes in transpiration rate. Where estimates of
419 stand transpiration are required by forestry, mining and land and water resource managers, with
420 limited access to sapflow data, but access to simple meteorological and soil moisture data, this
421 approach offers a reasonable estimation of water use, thereby assisting in the determination of water
422 balances for salinity control, water resource planning, vegetation management in relation to
423 groundwater management and impact assessments of mining and rehabilitation.

424

425 **Acknowledgements**

426

427 Weather data were provided by the NSW Department of Agriculture. This project was conducted in
428 collaboration with the State Forests of New South Wales and the NSW Department of Agriculture.
429 We thank the Cudmores family for providing access to their property (Paringa). Funding was
430 provided by the CRC for Greenhouse Accounting and the Australian Research Council. We thank
431 Dr Belinda Medlyn for timely discussion and input to the revised version of this Manuscript.

432

433

434 **References**

435

436 Banks R (1998) Soil landscapes of the Blackville 1:1000 000 sheet. Department of Land and Water
437 Conservation, Gunnedah.

438 David TS, Ferreira MI, David JS, Pereira JS (1997) Transpiration from a mature *Eucalyptus*
439 *globulus* plantation in Portugal during a spring-summer period of progressively higher water
440 deficit. *Oecologia* 110, 153-159.

441 Dolman AJ, Gash JHC, Roberts J and JSW (1991) Stomatal and surface conductance of tropical
442 rainforest. *Agric For Meteorol* 54, 303-313.

443 Eamus D, Hatton T, Cook P and Colvin C (2006) *Ecohydrology: vegetation function, water and*
444 *resource management*. CSIRO Press, Melbourne. 348 pp.

445 Eamus D, Hutley, LB, O'Grady AP (2001) Daily and seasonal patterns of carbon and water fluxes
446 above a north Australian savanna. *Tree Phys* 21, 977-988.

447 Eamus D, Shanahan S (2002) A rate equation model of stomatal responses to vapour pressure deficit
448 and drought. *BMC Ecol* 2, 1-14.

449 Ewers BE, Oren R (2000) Analyses of assumptions and errors in the calculation of stomatal
450 conductance from sap flux measurements. *Tree Phys* 20, 579-589.

451 Ewers BE, Mackay DS, Samanta S (2007) Interannual consistency in canopy stomatal conductance
452 control of leaf water potential across seven species. *Tree Phys* 27, 11-24.

453 Gash JHC, Shuttleworth WJ, Lloyd CR, Andre JC, Goutorbe JP, Gelpe J (1989)
454 Micrometeorological measurements in Les Landes forest during hapex-mobilhy. *Agric For*
455 *Met* 46, 131-147.

456 Granier A, Biron P, Leoine D (2000) Water balance, transpiration and canopy conductance in two
457 beech stands. *Agric For Met* 100, 291-308.

458 Harris PP, Huntingford C, Cox PM, Gasha JHC, Malhi Y (2004) Effect of soil moisture on canopy
459 conductance of Amazonian rainforest. *Agric For Met* 122, 215–227.

460 Howe P, Cook PG, O'Grady AP, Hillier J (2005) Pioneer Valley Groundwater Consultancy 3:
461 Analysis of Groundwater Dependent Ecosystem requirements. In Report for the Queensland
462 of Natural Resources and Mining. p. 117. Resource and Environmental Management Pty
463 Ltd.

464 Jarvis PG (1976) The interpretation of the variations in leaf water potential and stomatal
465 conductance found in canopies in the field. *Phil. Trans. R. Soc. Lond. B* 273, 593-610.

466 Kelliher FM, Leuning R, Schulze ED (1993) Evaporation and canopy characteristics of coniferous
467 forests and grasslands. *Oecologia* 95, 153-163.

468 Komatsu H, Kang Y, Kume T, Yoshifuji N, Hotta N (2006a) Transpiration from a *Cryptomeria*
469 *japonica* plantation, part 1: aerodynamic control of transpiration. *Hydrol Process* 20, 1309-
470 1320.

471 Komatsu H, Kang Y, Kume T, Yoshifuji N, Hotta N (2006b) Transpiration from a *Cryptomeria*
472 *japonica* plantation, part 2: responses of canopy conductance to meteorological factors.
473 *Hydrol Process* 20, 1321-1334.

474 Kosugi Y, Takanashi S, Tanaka H, Ohkubo S, Tani M, Yano M, Katayama T (2007)
475 Evapotranspiration over a Japanese cypress forest. I. Eddy covariance fluxes and surface
476 conductance characteristics for 3 years. *J Hydrol* 337, 269-283.

477 Lagergren F, Lindroth A (2002) Transpiration response to soil moisture in pine and spruce trees in
478 Sweden. *Agric For Met* 112, 67-85.

479 Lu P, Yunusa IAM, Walker RR, Muller WJ (2003) Regulation of canopy conductance and
480 transpiration and their modelling in irrigated grapevines. *Funct Pl Biol* 30, 689-698.

481 Lagergren F, Lindroth A (2002) Transpiration response to soil moisture in pine and spruce trees in
482 Sweden. *Agric and For Met* 112, 229 – 243.

483 Lundblad M, Lindroth A (2002) Stand transpiration and sapflow density in relation to weather, soil
484 moisture and stand characteristics. *Basic Appl Ecol* 3, 229-243.

485 Magnani F, Leonardi S, Tognetti R, Grace J, Borghetti M (1998) Modelling the surface conductance
486 of a broad-leaf canopy: effects of partial decoupling from the atmosphere. *Pl Cell Environ*
487 21, 867-879.

488 Medhurst JL, Battaglia M, Beadle CL (2002) Measured and predicted changes in tree and stand
489 water use following high intensity thinning of an 8 year old *E. nitens* plantation. *Tree Phys*
490 22, 775-784.

491 Monteith JL (1995) A reinterpretation of stomatal responses to humidity. *Plant Cell Environ* 18,
492 357-364.

493 O’Grady AP, Eamus D, Cook PG, Lamontagne S (2006) Groundwater use by riparian vegetation in
494 the wet-dry tropics of northern Australia. *Aust J Bot* 54, 145-154.

495 O’Grady AP, Eamus D, Hutley LH (1999) Transpiration increases in the dry season: patterns of tree
496 water use in the eucalypt open forests of northern Australia. *Tree Phys* 19, 591-597.

497 Ogink-Hendriks MJ (1995) Modelling surface conductance and transpiration of an oak forest in The
498 Netherlands. *Agric For Met* 74, 99-118.

499 Pataki DE, Oren R (2003) Species differences in stomatal control of water loss at the canopy scale
500 in a mature bottomland deciduous forest. *Adv in Water Resources* 26, 1267-1278.

501 Pataki DE, Oren R and Smith WK (2000) Sapflux of co-occurring species in a western subalpine
502 forest during seasonal soil drought. *Ecology* 81, 2557 – 2566.

503 Richardson AD, Hollinger DY (2005) Statistical modelling of ecosystem respiration using eddy
504 covariance data: Maximum likelihood parameter estimation, and Monte Carlo simulation of
505 model and parameter uncertainty, applied to three simple models. *Agric For Met* 131, 191-
506 208.

507 Rana G, Katerji N, de Lorenzi F (2005) Measurement and modelling of evapotranspiration of
508 irrigated citrus orchard under Mediterranean conditions. *Agric and For Met* 128, 199-209.

509 Rollenbeck R, Dieter A (2007) Characteristics of the water and energy balance in an Amazonian
510 lowland rainforest in Venezuela and the impact of the ENSO-cycle. *J Hydrol* 337, 377-390.

511 San Jose JJ, Nikonova N, Bracho R (1998) Comparison of factors affecting water transfer in a
512 cultivated paleotropical grass and a neotropoical savanna during the dry season of the
513 Orinoco lowlands. *J of Appl Met* 37, 509-522.

514 Simonin K, Kolb TE, Montes-Helu M, Koch G W (2007) The influence of thinning on
515 components of stand water balance in a ponderosa pine forest stand during and after extreme
516 drought. *Agric For Met* 143, 266-276.

517 Sommer R, de Abreu TD, Vielhauer K, de Araujo AC, Folster H, Vlek PLG (2002) Transpiration
518 and canopy conductance of secondary vegetation in the eastern Amazon. *Agric For Met* 112,
519 103-121.

520 Stewart JB (1988) Modelling surface conductance of pine forest. *Agric For Met* 43, 19-35.

521 Thomas DS and Eamus D (1999) The influence of predawn leaf water potential on stomatal
522 responses to atmospheric water content at constant C_i and on stem hydraulic conductance
523 and foliar ABA concentrations. *J Exp Bot* 50, 243-251.

524 Thomas DS, Eamus D, Shanahan S (2000) Influence of season, drought and xylem ABA on
525 stomatal responses to leaf-to-air vapour pressure difference of trees of the Australian wet-dry
526 tropics. *Aust J Bot* 48, 143-151.

527 Whitehead D (1998) Regulation of stomatal conductance and transpiration in forest canopies. *Tree*
528 *Phys* 18, 633-644.

529 Williams M, Malhi Y, Nobre A, Rastetter E, Grace J, Pereira M (1998) Seasonal variation in net
530 carbon exchange and evapotranspiration in a Brazilian rain forest. *Plant Cell Environ* 21,
531 953-968.

532 Wright IR, Manzi AO, da Rocha HR (1995) Surface conductance of Amazonian pasture: model
533 application and calibration for canopy climate. *Agric For Met* 75, 51-70.

534 Wullschleger SD, Wilson KB, Hanson PJ (2000) Environmental control of whole plant
535 transpiration, canopy conductance and estimates of the decoupling coefficient for large red
536 maple trees. *Agric and Fore Met* 104, 157-168.

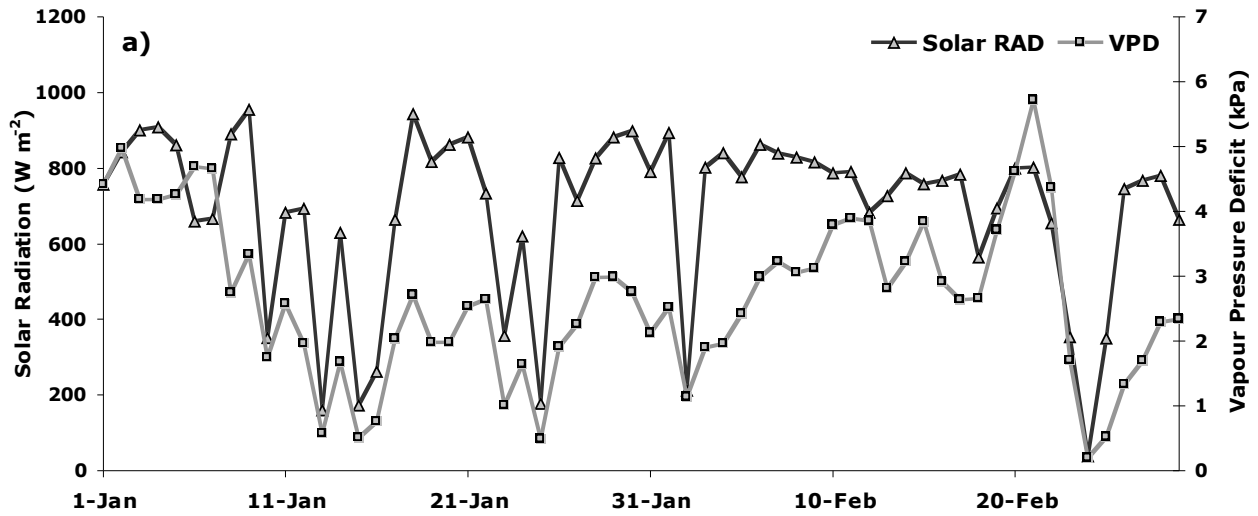
537 Wullschleger SD, FC, Meinzer, RA Vertessey (1998). A review of whole-plant water use studies in
538 trees. *Tree Phys* 18, 499-512.

539 Wullschleger SD, Hanson PJ (2006) Sensitivity of canopy transpiration to altered precipitation in
540 an upland oak forest: evidence from a long-term field manipulation study. *Glob Change Biol*
541 12, 97-109.

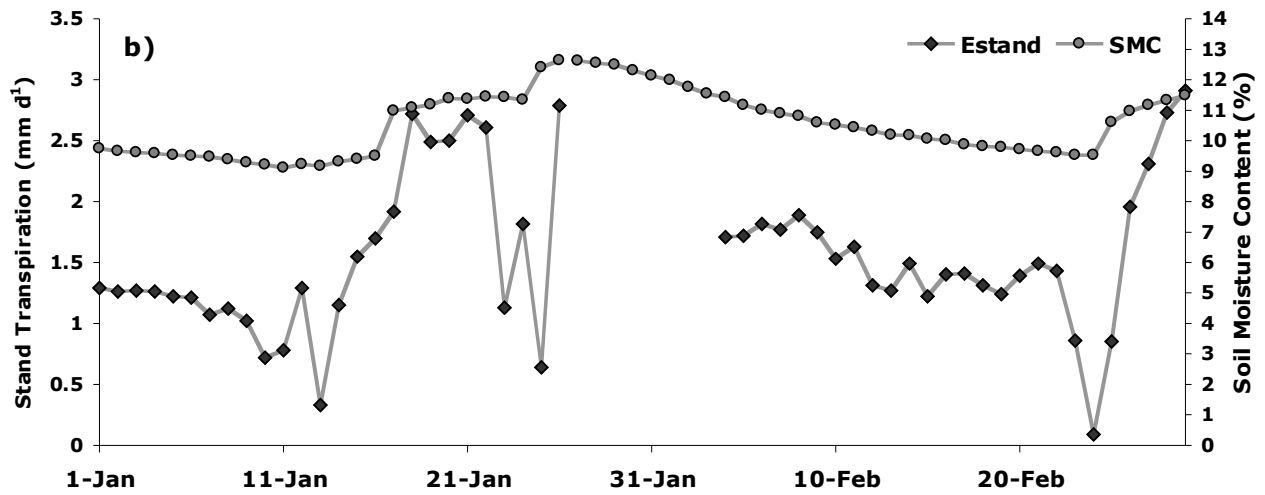
542 Zeppel MJ (2006) The influence of drought and other abiotic factors on tree water use in a temperate
543 remnant forest. PhD Thesis. University of Technology Sydney.

544 Zeppel MJB, Eamus D (2005) Tree water use under conditions of drought. *Agric Sci* 17, 8-11.

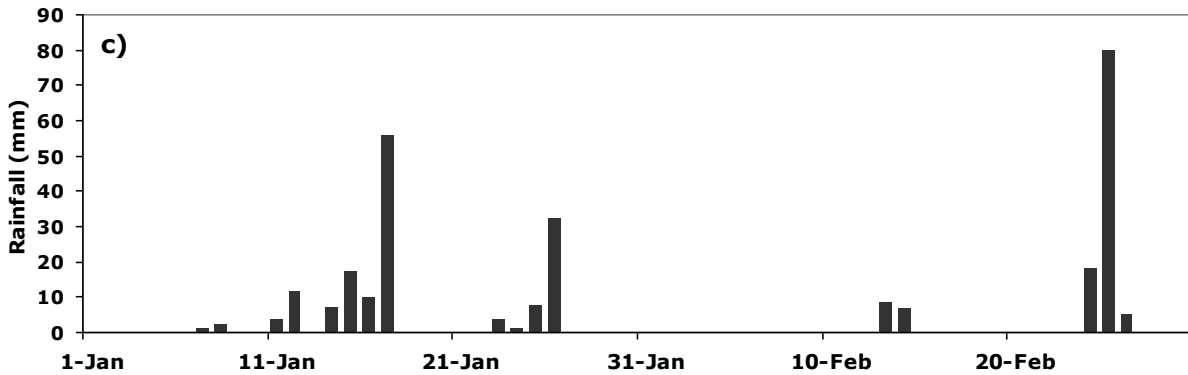
- 545 Zeppel MJB, Murray BR, Barton C, Eamus D (2004) Seasonal responses of xylem sap velocity to
546 VPD and solar radiation during drought in a stand of native trees in temperate Australia.
547 *Funct Plant Biol* 31, 461-470.
- 548 Zhang H, Simmonds L P, Morison J I L, Payne D and Wullschleger 1997 Estimation of transpiration
549 by single trees: comparison of sap flow measurements with a combination equation. *Agric*
550 *For Met* 87, 155-169.



551



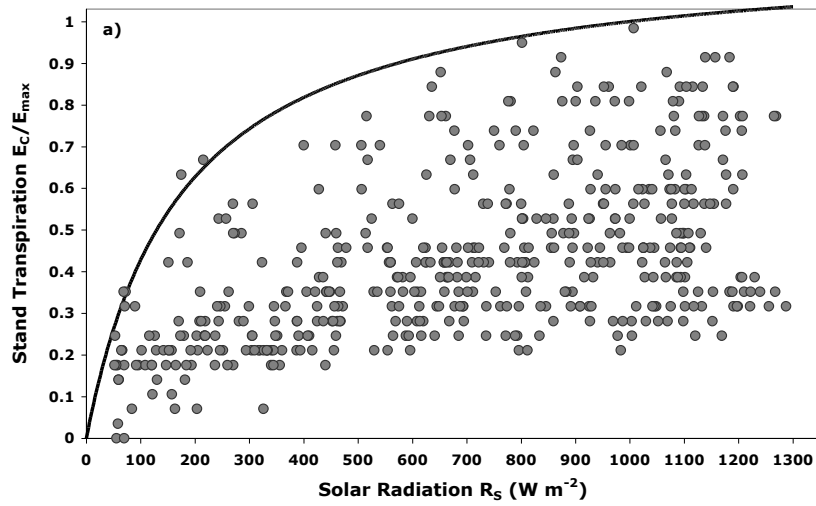
552



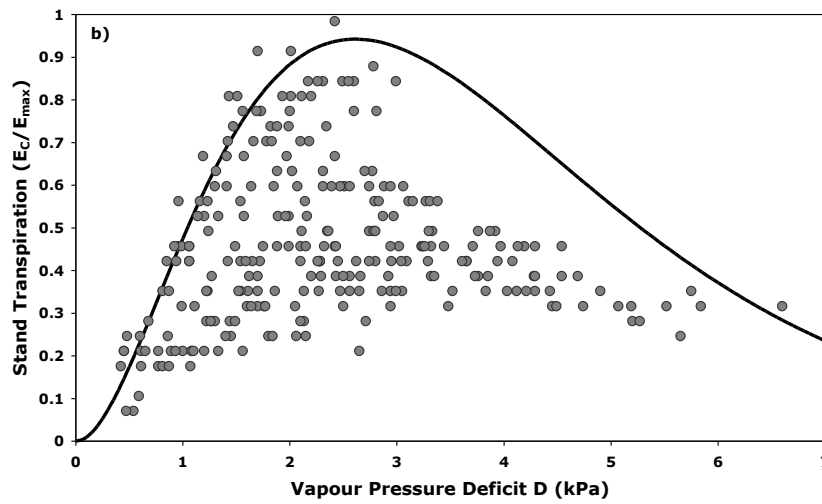
553
554
555
556
557
558
559

Figure 1 a) Comparisons between incident solar radiation (R_s), vapour pressure deficit (D), b) soil moisture content (θ), stand transpiration (E_c) and c) rainfall over the periods of January and February 2004. Diurnal changes in the three driving environmental variables R_s , D and θ shows a resulting change in E_c .

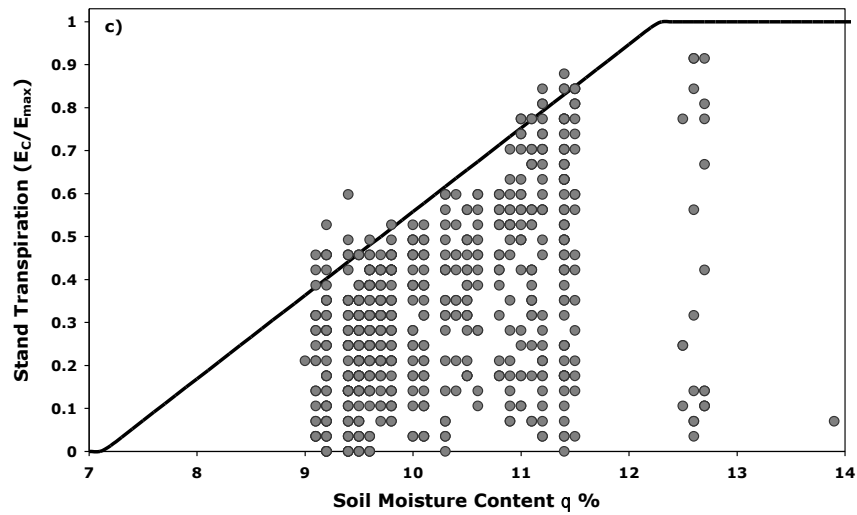
560



561



562



563

564

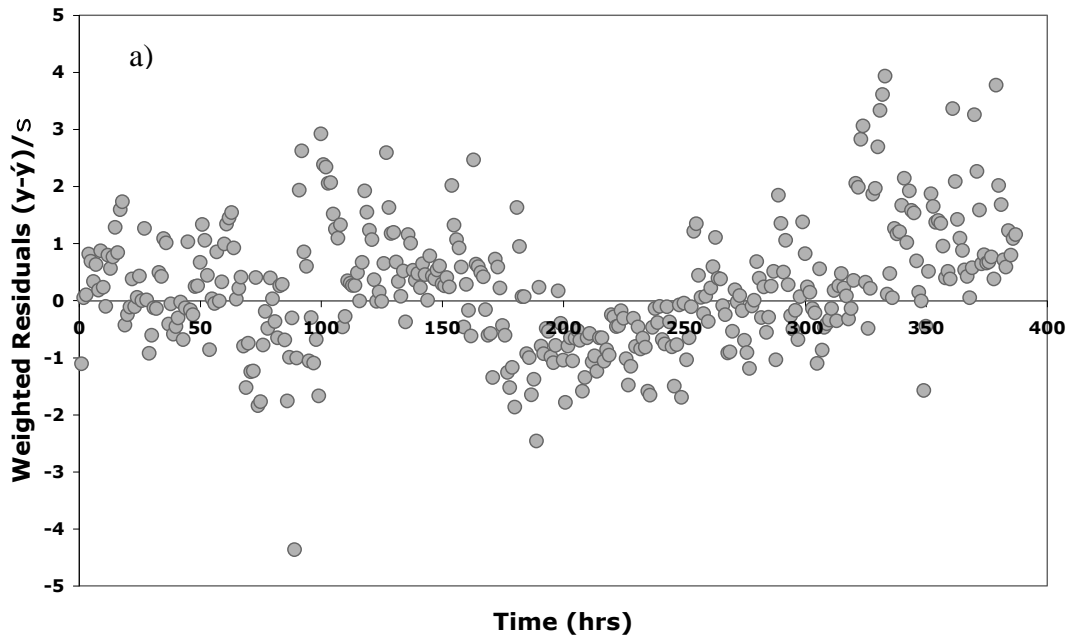
565

566

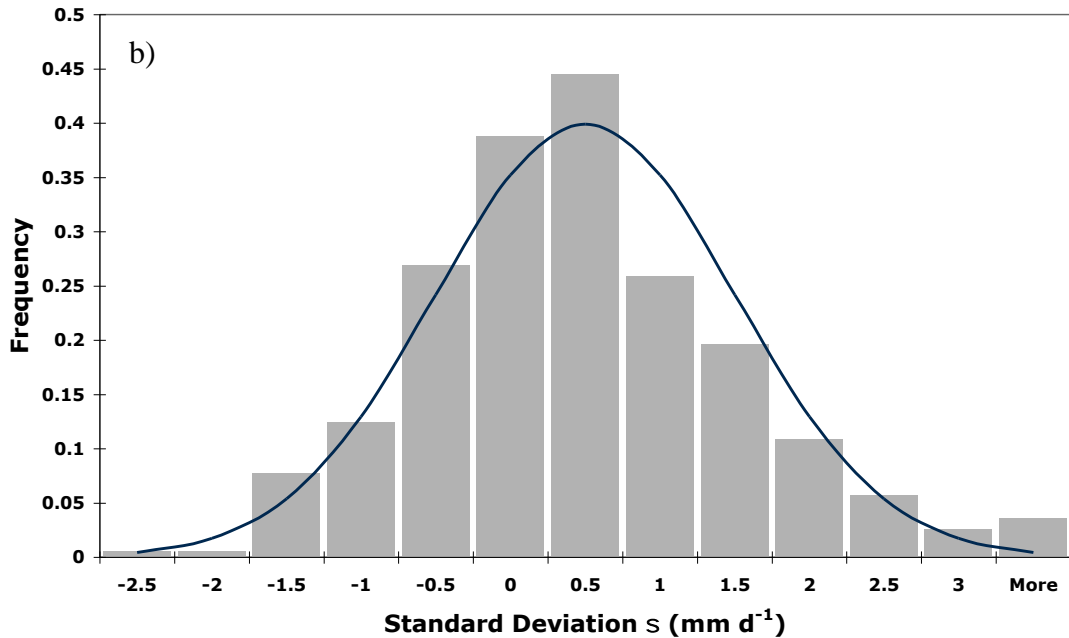
Figure 2:

The form of the environmental response functions for a) incident solar radiation (R_s), b) vapour pressure deficit (D) and c) soil moisture content (θ), with relation to the boundaries of the scattered data points.

567



568

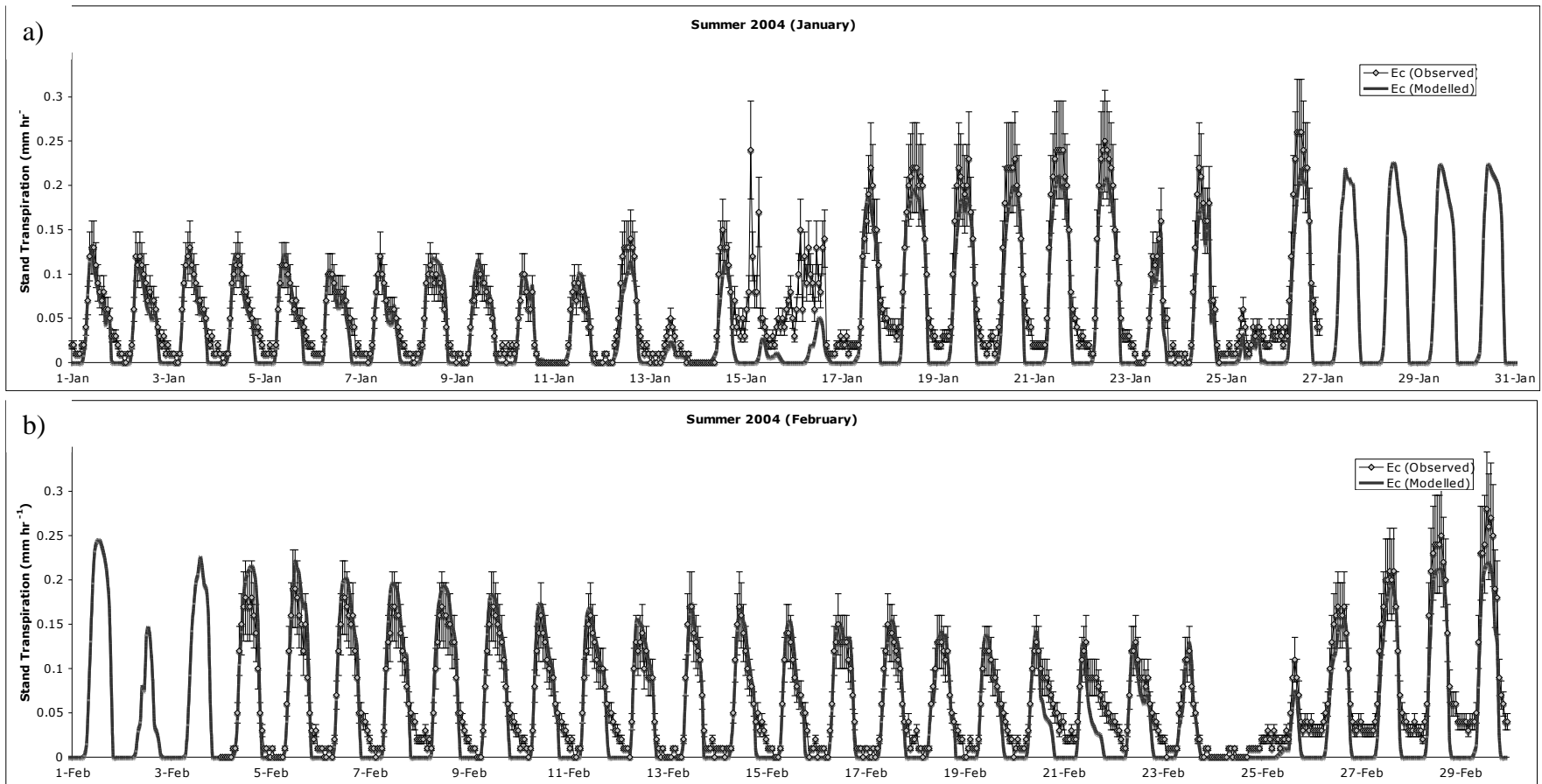


569
570
571
572
573
574
575
576

Figure 3:

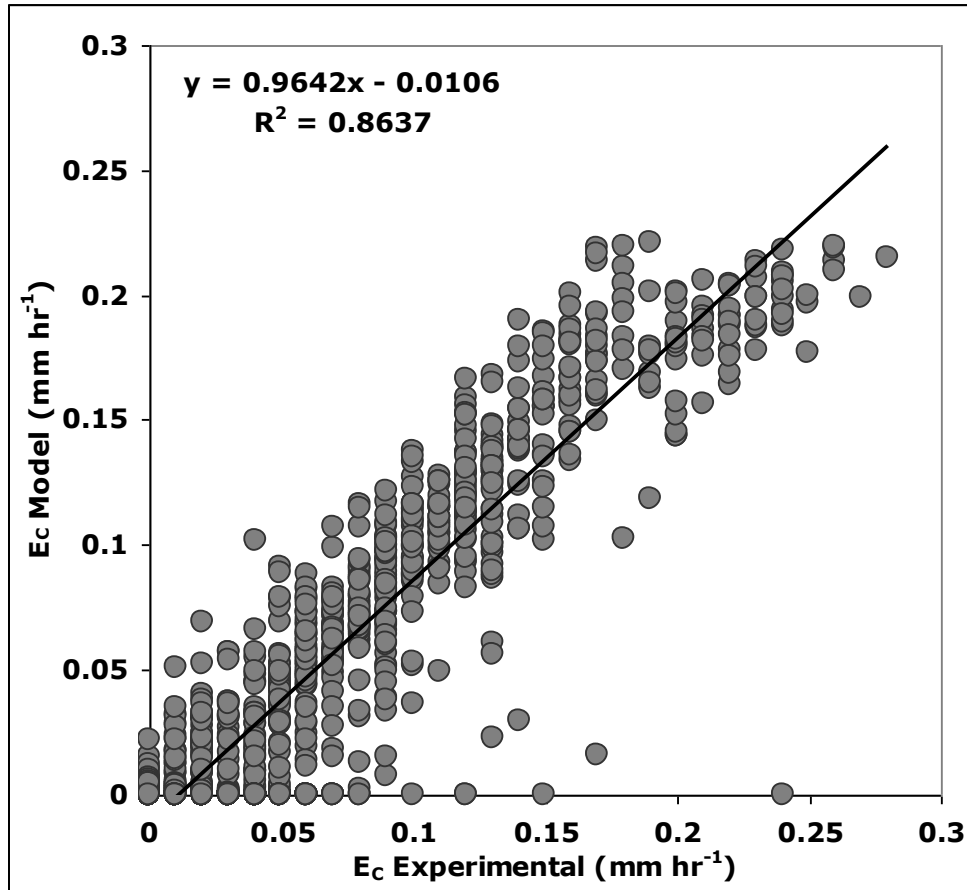
Weighted residuals expressed in terms of standard deviations for the modified Jarvis model showing a slightly sinusoidal pattern in the residuals (a). The dashed lines show the regions for which the residuals fall between ± 1 standard deviations, representative of a 68% confidence region. The distribution of weighted residuals assuming a normal assuming a Gaussian distribution (b), where the residuals are evenly distributed within the 68% confidence region or ± 1 standard deviations.

577



578
579
580
581
582
583
584
585

Figure 4: Estimated stand transpiration compared with field data over the 2 month period of a) January and b) February 2004. The model output is in good agreement with the observed measurements; uncertainty in the measurements is indicated by the error bars.



587
 588
 589
 590
 591
 592
 593
 594
 595
 596
 597
 598
 599
 600
 601
 602
 603

Figure 5: Comparison between estimated and observed stand transpiration, including the increasing uncertainty in the measurements (dotted lines). The slope corresponds to a value of 0.96 and an $R^2 = 0.90$.

604
605
606
607
608
609
610
611
612

Table 1:

Parameters from the optimisation of the modified Jarvis model estimating stand transpiration for an Australia native forest for a weighted nonlinear least squares regime. Parameters defined a maximum stand transpiration (E_{max}), environmental functional dependencies on solar radiation (k_1), vapour pressure deficit (k_2, k_3), soil moisture content at wilting (θ_w), and critical points (θ_C).

	Value	S.E
E_{max}	0.260	0.004
k_1	143.40	19.43
k_2	0.917	0.016
k_3	1.372	0.010
θ_w	6.72	0.16
θ_C	11.79	0.09
β	0.23	
WSSR	128.55	
AIC	920.13	
R²	0.90	

613
614
615